Circulation

ORIGINAL RESEARCH ARTICLE

Virus-Induced Acute Respiratory Distress Syndrome Causes Cardiomyopathy Through Eliciting Inflammatory Responses in the Heart

Jana Grune, PhD; Geetika Bajpai, PhD; Pervin Tülin Ocak, Eva Kaufmann, DVM, PhD; Kyle Mentkowski, PhD; Steffen Pabel, MD; Nina Kumowski, MD; Fadi E. Pulous, PhD; Kim A. Tran, David Rohde, MD; Shuang Zhang, PhD; Yoshiko Iwamoto, BS; Gregory R. Wojtkiewicz, MS; Claudio Vinegoni, PhD; Ursula Green; Filip K. Swirski, PhD; James R. Stone, MD; Jochen K. Lennerz, MD; Maziar Divangahi, PhD; Maarten Hulsmans, PhD; Matthias Nahrendorf, MD, PhD

BACKGROUND: Viral infections can cause acute respiratory distress syndrome (ARDS), systemic inflammation, and secondary cardiovascular complications. Lung macrophage subsets change during ARDS, but the role of heart macrophages in cardiac injury during viral ARDS remains unknown. Here we investigate how immune signals typical for viral ARDS affect cardiac macrophage subsets, cardiovascular health, and systemic inflammation.

METHODS: We assessed cardiac macrophage subsets using immunofluorescence histology of autopsy specimens from 21 patients with COVID-19 with SARS-CoV-2–associated ARDS and 33 patients who died from other causes. In mice, we compared cardiac immune cell dynamics after SARS-CoV-2 infection with ARDS induced by intratracheal instillation of Toll-like receptor ligands and an ACE2 (angiotensin-converting enzyme 2) inhibitor.

RESULTS: In humans, SARS-CoV-2 increased total cardiac macrophage counts and led to a higher proportion of CCR2$^+$ (C-C chemokine receptor type 2 positive) macrophages. In mice, SARS-CoV-2 and virus-free lung injury triggered profound remodeling of cardiac resident macrophages, recapitulating the clinical expansion of CCR2$^+$ macrophages. Treating mice exposed to virus-like ARDS with a tumor necrosis factor α–neutralizing antibody reduced cardiac monocytes and inflammatory MHCII^{lo} CCR2$^+$ macrophages while also preserving cardiac function. Virus-like ARDS elevated mortality in mice with pre-existing heart failure.

CONCLUSIONS: Our data suggest that viral ARDS promotes cardiac inflammation by expanding the CCR2$^+$ macrophage subset, and the associated cardiac phenotypes in mice can be elicited by activating the host immune system even without viral presence in the heart.

Key Words: acute respiratory distress syndrome ■ CCR2 ■ macrophage ■ SARS-CoV-2

During recurring seasonal waves, respiratory viral infections cause endemic and pandemic threats, ranging from mild flu-like symptoms to life-threatening acute respiratory distress syndrome (ARDS). A recent example has been SARS-CoV-2 causing COVID-19. In a subset of vulnerable patients, COVID-19 elicits ARDS with high mortality rates.[1] Although COVID-19 is considered primarily a respiratory disease, excessive systemic inflammation and a cytokine storm accompanied by high levels of circulating immune cells may occur.[2] The cytokine release by activated immune cells may contribute to myocardial injury, which is observed

Correspondence to: Matthias Nahrendorf, MD, PhD, Center for Systems Biology, Massachusetts General Hospital, Richard B. Simches Research Center, 185 Cambridge St, Suite 5.210, Boston, MA 02114, Email mnahrendorf@mgh.harvard.edu, or Jana Grune, PhD, Department of Cardiothoracic and Vascular Surgery, Deutsches Herzzentrum der Charité, Augustenburger Platz 1, 13353 Berlin, Germany, Email jana.grune@dhzc-charite.de
Supplemental Material is available at https://www.ahajournals.org/doi/suppl/10.1161/CIRCULATIONAHA.123.066433.
For Sources of Funding and Disclosures, see page XXX.

Circulation is available at www.ahajournals.org/journal/circ

Clinical Perspective

What Is New?

- Cardiac macrophage subsets change in patients with COVID-19 toward the inflammatory CCR2$^+$ (C-C chemokine receptor type 2 positive) subset.
- Cardiac phenotypes can be induced by activation of the immune system of the host even without viral presence in the heart.

What Are the Clinical Implications?

- Our data acquired in mice with virus-like acute respiratory distress syndrome support the idea that modulating the host immune response may alleviate inflammatory cardiac complications.
- CCR2$^+$ macrophages may serve as a therapeutic target to alleviate cardiovascular complications in vulnerable patients with viral infections.

Nonstandard Abbreviations and Acronyms

ACE2	angiotensin-converting enzyme 2
angII	angiotensin II
ARDS	acute respiratory distress syndrome
CCR2	C-C chemokine receptor type 2
HFpEF	heart failure with preserved ejection fraction
LPS	lipopolysaccharide
MyD88	myeloid differentiation primary response 88
IFN	interferon
TLR	Toll-like receptor
VLARDS	virus-like ARDS

in up to 50% of patients.[3] The underlying mechanisms are still a matter of debate. Because mortality rates rise among patients with cardiovascular and metabolic diseases such as hypertension, diabetes, and obesity, which are associated with immune activation, a primed immune system likely contributes to cardiovascular complications during viral infections. The risk of developing cardiac complications, including heart failure, myocarditis or pericarditis, remains elevated after recovery from the acute phase of viral infections, even among vaccinated patients who were not hospitalized,[4] emphasizing the importance of understanding the myocardial inflammatory response to viral respiratory infections.

Macrophage expansion is a feature of viral ARDS. Disease severity positively correlates with overall lung leukocyte numbers.[5] Bronchoalveolar lavage fluid samples from patients with severe COVID-19 revealed increased neutrophils, depleted tissue-resident alveolar macrophages, and abundant inflammatory monocyte-derived macrophages.[6] Cardiac macrophages can be divided into CCR2$^-$ (C-C chemokine receptor type 2 negative) and CCR2$^+$ subsets with divergent origins and functional identities.[7] CCR2$^+$ subsets are monocyte-derived and preferentially accumulate at sites of inflammation in response to tissue injury. Resident cardiac macrophage subsets are CCR2$^-$ and proliferate locally.[8] The roles of tissue-resident macrophages versus monocyte-derived macrophages during cardiac injury associated with viral ARDS, and specifically in SARS-CoV-2 infection, are less clear. In autopsies of patients with COVID-19, cardiac CD68$^+$ macrophage levels were expanded in 86% of 21 cases independent of disease severity.[9]

Here, we investigate how immune signals typical for virus-induced ARDS affect cardiovascular health, systemic inflammation, and macrophage subsets in cardiac autopsy specimens from patients with COVID-19 , in mice infected with SARS-CoV-2, and in uninfected mice with "virus-like ARDS" (^{VL}ARDS). In humans and mice, ARDS and systemic inflammation altered total cardiac macrophage counts and expanded the proportion of CCR2$^+$ macrophages. Currently, it remains unclear to what degree COVID-19–induced myocardial inflammation is caused by viral infection of the heart versus the systemic immune response of the host to the virus. To probe whether cardiac sequelae also occur in the absence of viral infection, we examined mouse cardiac leukocytes after inducing ARDS with TLR (Toll-like receptor) ligands and ACE2 (angiotensin-converting enzyme 2) inhibitor to mimic pathways activated by SARS-CoV-2 infections.[10–12] Lung injury in virus-free mice triggered profound remodeling of the resident macrophages of the heart and recapitulated the CCR2$^+$ macrophage expansion in patients with COVID-19. Our data suggest that cardiac inflammation and associated outcomes can be elicited by activating the immune system even without viral presence in the heart. In mice with ^{VL}ARDS, immunomodulatory therapeutics alleviated heart inflammation and preserved cardiac function.

METHODS

An extended methods section is provided in the Supplemental Material. The data that support the findings of this study are available from the corresponding author upon reasonable request. Autopsy specimens from controls (n=33) were collected between September and December 2019, before the global pandemic started, at the Pathology Department of Massachusetts General Hospital. The study was approved by an institutional review committee. All animal procedures were performed in accordance with the National Institutes of Health Guide for the Care and Use of Laboratory Animals and in accordance with the guidelines by the Canadian Council on Animal Care and approved by the institutional animal care and use committee and by the animal research ethics board of McGill University and Massachusetts General Hospital.

Statistical Analyses

Statistical analyses were performed using GraphPad Prism 9 (GraphPad Software, San Diego, CA). Results are reported as mean SEM. Normality was assessed using a Shapiro-Wilk normality test. For a 2-group comparison, normally distributed data sets underwent an unpaired parametric 2-tailed *t* test; not normally distributed data sets underwent a Mann-Whitney test. For multiple comparisons, normally distributed data sets underwent a 1-way or 2-way ANOVA followed by a Bonferroni multiple comparisons test as appropriate and indicated in the respective figure legends; not normally distributed data sets underwent a Kruskal-Wallis test followed by a Dunn multiple comparisons test. Categorical characteristics of the human cohort were tested using a Fisher exact test. There are no deposited data associated with this article.

RESULTS

^{VL}ARDS Mouse Model

We aimed to reproduce features of clinical SARS-CoV-2–associated ARDS in mice to test whether immune signaling typical for viral infections is sufficient to cause cardiac phenotypes seen in patients with COVID-19, even in the absence of the virus. Repeated saline lavage causes ARDS through surfactant depletion and mechanical injury.[13] Without additional stimuli, saline lavage leads to some impaired permeability but limited recruitment of immune cells.[14] Building on this model, we used daily intratracheal saline instillations to deliver immune-stimulatory agents that mimic signaling pathways activated by SARS-CoV-2 to establish sterile ^{VL}ARDS with pronounced systemic inflammation (Figure 1A). We used 150 µL of saline to deliver 4 components. First, we delivered the ACE2 inhibitor MLN4760. Type II alveolar epithelial cells express ACE2,[15] and coronaviruses use it as an entrance receptor.[16] SARS-CoV-2 spike proteins bind to and thus downregulate ACE2,[11] a phenomenon we mimic here by chemical ACE2 inhibition. ACE2 inactivates angII (angiotensin II) and negatively regulates angII production. SARS-CoV-2–associated ACE2 downregulation leads to excessive angII production that promotes lung injury[17] and cardiovascular complications.[18] Second, we delivered the TLR7 and 8 agonists resiquimod and imiquimod to mimic endosomal TLR7 and TLR8 receptor activation by viral DNA.[10] Ligating these TLRs initiates a type I IFN (interferon) response that activates MyD88 (myeloid differentiation primary response 88) signaling and downstream proinflammatory cytokine production, thereby conferring antiviral protection to the host. Third, we delivered the prototypical TLR4 agonist LPS (lipopolysaccharide). TLR4 activation can result from bacterial coinfections that frequently occur in patients with ARDS.[19] The viral spike protein is being discussed as a potential TLR4 ligand.[20] No matter whether parts of the virus or bacterial components ligate the receptor, it has become clear that TLR4 activation plays a role in triggering the cytokine storm after SARS-CoV-2 infection.[21]

Mice with ^{VL}ARDS lost body weight over the time period of the 5 daily intratracheal instillations (Figure 1B). Body temperature was lower in ^{VL}ARDS mice (Figure 1C), indicating hypothermia, a feature of both ARDS and septic shock. The mortality rate was >40% in mice with ^{VL}ARDS on day 5 of the experiment (Figure 1D), an outcome that matches clinical ARDS mortality.[22] Computed tomography of the lungs revealed bilateral opacities and lung infiltrations (Figure 1E and 1F). Mice with ^{VL}ARDS had diminished blood oxygenation (Figure 1G), which also signifies ARDS. ^{VL}ARDS increased D-dimers, reduced blood pressure, and lowered heart rates (Figure S1A through S1E), whereas neutrophils and monocytes rose in circulation (Figure S1G and S1H).

Leukocyte Recruitment and Lung Inflammation During ^{VL}ARDS

At steady-state, lungs harbor alveolar macrophages and monocyte-derived macrophages.[23] The latter are rapidly recruited from the circulation during ARDS. Histological staining revealed diffuse alveolar damage and cellular infiltration in ^{VL}ARDS compared with control mice (Figure 1H). CD45$^+$ leukocytes increased in lungs of mice with ^{VL}ARDS, an expansion driven by influx of neutrophils and monocyte-derived macrophages (Figure 1I and 1J). As expected, alveolar macrophages were reduced in ^{VL}ARDS mice (Figure 1I and 1J), suggesting the death of this cell population. Macrophage activation leads to release of IFNγ, tumor necrosis factor α (TNFα), and interleukin 10 (IL10) in the setting of SARS-CoV-2 infection.[24] Expression of *Il1β*, *Il6*, *Il10*, *Cxcl2*, *Ifnγ*, and *TNFα* was upregulated in ^{VL}ARDS lungs compared with control lungs, indicating that delivering the immune stimulants in the ARDS cocktail elicited the predicted phenotype (Figure 1K). This was further supported by elevated serum protein levels of IL6 (Figure 1L), IL1ß, IFNγ, and TNFα (Figure S1I). Il1ß and Il6 proteins were also augmented in the bronchoalveolar lavage fluid from mice with ^{VL}ARDS (Figure 1M). Heightened IL6 levels are associated with COVID-19 severity and adverse outcomes.[25] Effects of ^{VL}ARDS were similar in male and female mice (Figure 1J and 1L). Together, these data show that ^{VL}ARDS phenocopies inflammatory pathways that are active in ARDS associated with SARS-CoV-2.

^{VL}ARDS Induces a Phenotypic Switch Among Cardiac Macrophage Subsets

A key feature of SARS-CoV-2–induced ARDS is systemic inflammation, as evidenced by blood neutrophilia and monocytosis and dysregulated cytokine and chemokine profiles.[25] Excessive inflammation can cause organ damage or failure and cause cardiac complications such

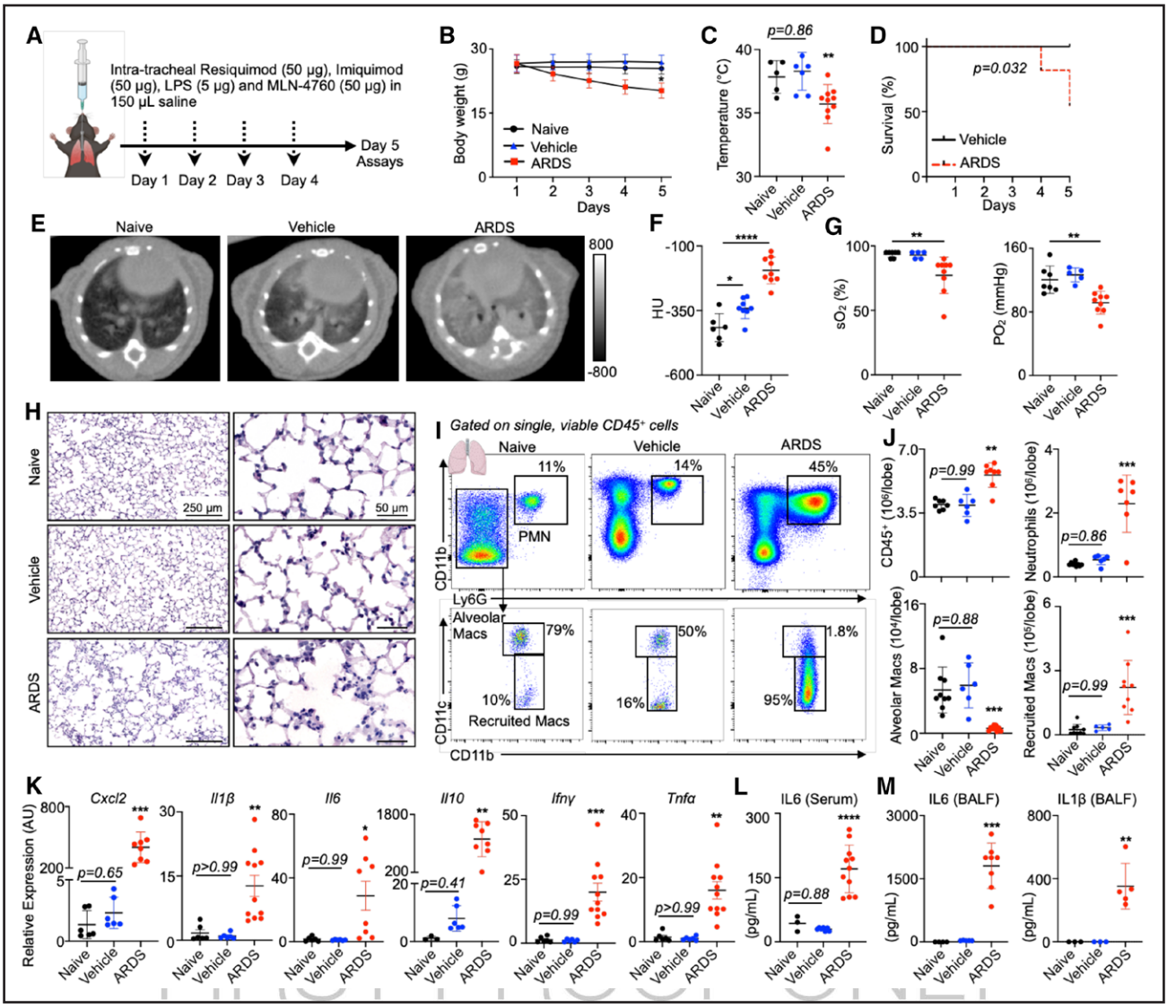

Figure 1. A mouse model of ^{VL}ARDS.

A, Experimental outline. All assays were done on day 5 after the first instillation. **B**, Body weight in grams (n=6 mice per group). **C**, Body temperature (°C). **D**, Kaplan-Meier curve indicating mortality of ^{VL}ARDS (n=11) and vehicle-treated control (n=8 mice, log rank Mantel-Cox test. **E**, X-ray computed tomography images and lung opacity quantification (**F**) reported in Hounsfield units (HU). **G**, sO2 and PaO2 in arterial blood. **H**, Lung H&E staining indicating increased cellularity in lungs of mice with ARDS. Scale bars=250 µm (**left**) and 50 µm (**right**). **I**, Representative flow plots for lung tissue and corresponding quantification of leukocyte, neutrophil, and macrophage counts per lung lobe (**J**). **K**, qRT-PCR analysis of total lung tissue. **L**, ELISA for IL6 in serum. **M**, ELISA for IL6 and IL1ß in bronchoalveolar lavage fluid (BALF). *P<0.05; **P<0.01; ***P<0.001; ****P<0.0001 vs naive control group. One-way ANOVA followed by Bonferroni multiple comparisons test or Kruskal-Wallis test followed by Dunn multiple comparisons test, as appropriate. Data are mean±SEM. ARDS indicates acute respiratory distress syndrome; LPS, lipopolysaccharide; and ^{VL}ARDS, virus-like ARDS.

as acute myocardial injury, myocarditis, arrhythmias, or thromboembolism.[26] To test whether ^{VL}ARDS affects cardiac function, we performed echocardiography. We found a reduced ejection fraction, stroke volume, and cardiac output in mice with ^{VL}ARDS compared with controls (Figure 2A through 2C), results that suggest loss of systolic function. On day 5 after ^{VL}ARDS induction, blood troponin levels increased (Figure 2D).

Although patients with SARS-CoV-2 have more heart macrophages,[9] the role of macrophages and their subsets in this context is not clear. Subset shifting could be of importance because certain cardiac macrophage subsets support cardiomyocyte metabolism[27] and preserve normal conduction.[28] Histology of mouse cardiac sections revealed cellular infiltrations in left ventricular myocardium of mice with ^{VL}ARDS (Figure 2E). Flow cytometry revealed neutrophil and monocyte recruitment to the heart, which peaked on days 5 and 3, respectively (Figure 2F through 2H). Overall cardiac macrophage counts also increased on day 5 in mice with ^{VL}ARDS (Figure 2H). In ^{VL}ARDS mice, MHCII^{hi} CCR2^{+} and MHCII^{hi} CCR2^{-} macrophage subsets were reduced on day 3 and

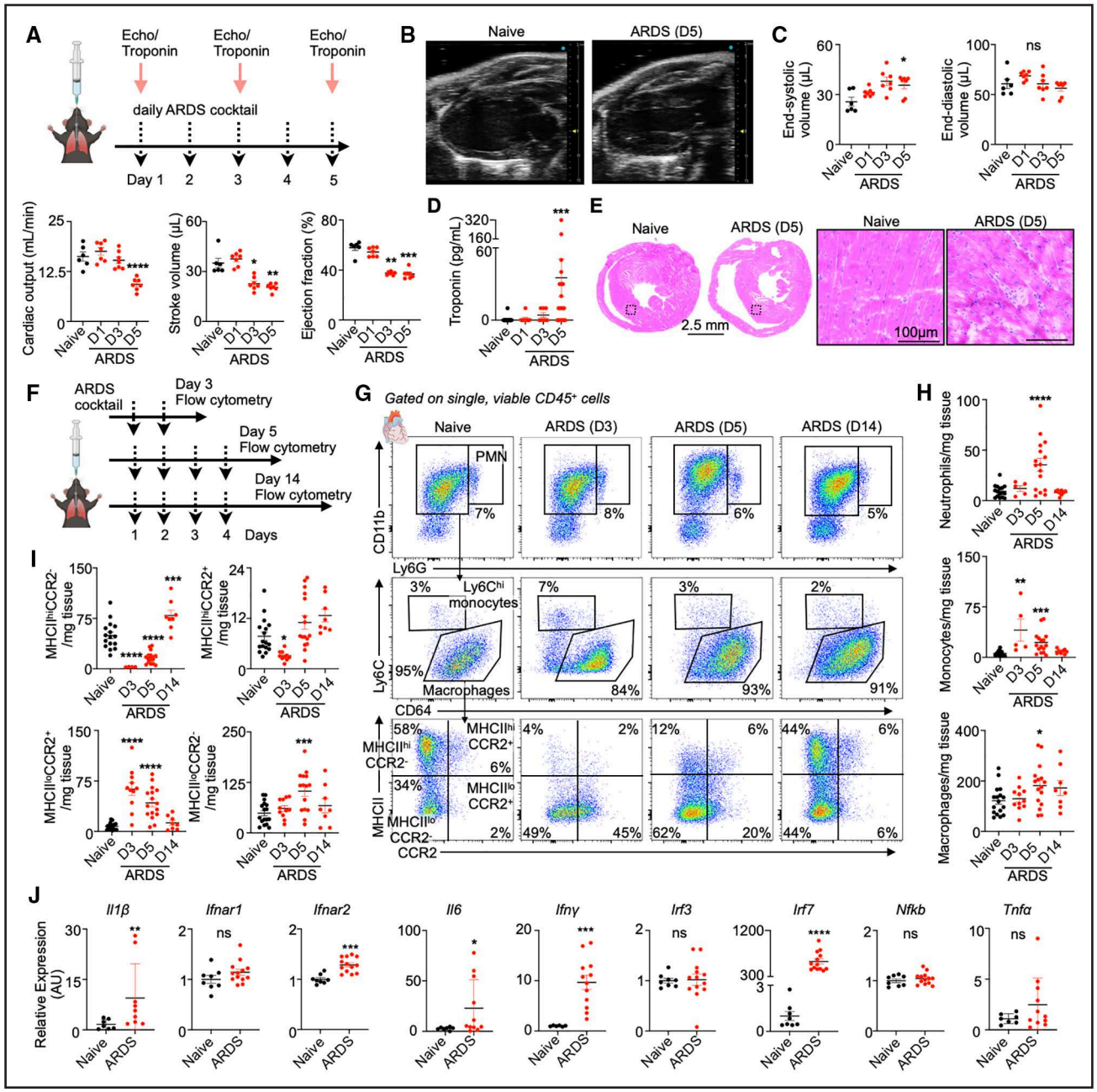

Figure 2. Phenotypic changes of cardiac macrophage subsets in ^{VL}ARDS.

A, Experimental outline. **B**, B-mode images of the left ventricle in a parasternal long-axis view and quantitative analyses (**C**). **D**, Troponin levels measured in whole blood samples. **E**, H&E-stained cardiac cross-sections and 20× magnifications demonstrating cellular infiltration. Scale bar=2.5 mm (**left**) or 100 µm (**right**). **F**, Experimental outline. Flow cytometry was performed on days 3, 5, and 14 after the first instillation. **G**, Exemplary flow plots of cardiac tissue. **H**, Quantification of leukocyte populations and macrophage subsets (**I**) in hearts from naive and ^{VL}ARDS mice. One-way ANOVA followed by Bonferroni multiple comparisons test or Kruskal-Wallis test followed by Dunn multiple comparisons test, as appropriate. **J**, qRT-PCR analyses of bulk heart tissue on day 5 after first instillation. Unpaired parametric 2-tailed *t* test or Mann-Whitney test, as appropriate. **P*<0.05; ***P*<0.01; ****P*<0.001; *****P*<0.0001 vs naive control group. Data are mean±SEM. ARDS indicates acute respiratory distress syndrome; CCR2, C-C chemokine receptor type 2; and ^{VL}ARDS, virus-like ARDS.

then recovered rapidly (Figure 2I). MHCII^{lo} CCR2^{+} macrophages, which are not present in the steady-state heart and are thought to have an inflammatory phenotype,[29] expanded on days 3 and 5 after ^{VL}ARDS induction (Figure 2I). MHCII^{lo} CCR2^{-} macrophages peaked on day 5 (Figure 2I). The decline of some myocardial macrophage subsets may be caused by their death, as we detected increased numbers of TUNEL^{+} CD68^{+} macrophages on day 3 after ^{VL}ARDS induction (Figure S2A through S2C). Macrophage subset perturbations were accompanied by higher myocardial expression of *Il1β*, *Il6*, *Ifnγ*, *Ifnar2*, and *Irf7* (Figure 2J).

To decipher to which degree TLR4 signaling contributed to the observed innate immune changes, we subjected cohorts of mice to a ^{VL}ARDS regimen that lacked LPS and to LPS-only instillations, comparing with naive mice and mice that received the complete ^{VL}ARDS cocktail (Figure S2D). We found that in blood, LPS was responsible for the increase in neutrophils, which did not occur if LPS was lacking from the ARDS cocktail, whereas blood monocyte subsets were not significantly dependent on LPS (Figure S2E). In the myocardium, overall macrophage numbers increased no matter whether LPS was present in the ARDS cocktail (Figure S2F). LPS increased the numbers of neutrophils and monocytes in the myocardium (Figure S2F). LPS did not influence depletion of resident MHCII^{+} Ccr2^{-} macrophages but augmented numbers of recruited MHCII^{hi} Ccr2^{+} macrophages (Figure S2F), which aligns with increased myocardial monocyte numbers. Taken together, TLR4 signaling mostly influenced neutrophil and monocyte recruitment to the heart.

To compare leukocyte fluctuations after ^{VL}ARDS induction with infection with the SARS-CoV-2 virus, we pursued experiments in CoV-2–susceptible *K18-hACE2* mice (Figure S3A). Regardless of viral presence, we observed an increase of interstitial macrophages and a reduction of alveolar macrophages in the lung, which was more pronounced in ^{VL}ARDS mice (Figure S3B). Fluorescence-activated cell sorting analysis of the heart showed an increase of heart macrophages in both models, which was more pronounced in SARS-CoV-2–infected mice (Figure S3C). Cardiac macrophage subsets were altered similarly in both models, with the exception of MHCII^{hi} Ccr2^{-} macrophages. This resident subset only decreased in ^{VL}ARDS mice (Figure S3C). To begin exploring this divergence, we pursued quantitative real-time PCR analysis of the myocardium in both models, which showed a significantly higher upregulation of *Ifny* and *Tnfα* in ^{VL}ARDS myocardium (Figure S3D). We speculate that a strong TLR7/8 ligation in ^{VL}ARDS mice may have depleted MHCII^{hi} Ccr2^{-} macrophages in the heart. Of note, Ifny is a potent activator of macrophages and typically increases expression of MHCII,[30] making it less likely that the above finding was caused by cellular downregulation of MHCII.

To address how the observed neutrophilia after ^{VL}ARDS induction affects cardiac dysfunction, we depleted neutrophils with neutralizing antibodies (Figure S4A and S4B). We observed that neutrophil depletion did not affect cardiac macrophage counts and blood troponin levels (Figure S4C through S4E). Neutrophil depletion preserved the ejection fraction measured by echocardiography (Figure S4F).

SARS-CoV-2–Associated ARDS Disrupts Cardiac Macrophage Subsets in Patients

To test whether cardiac macrophage subsets change in patients, we stained for macrophage markers CD68 and CCR2 in myocardial autopsy specimens from 21 patients with a confirmed COVID-19 infection leading to SARS-CoV-2–associated ARDS (Table; Table S1; Figure 3A; Figure S5). For comparison, 33 patients who died from non–COVID-19 causes before the pandemic served as controls. CD68^{+} macrophages were more abundant in patients with COVID-19 than in controls (Figure 3B), matching a previous report.[9] In line with our findings in mice, the recruited CCR2^{+} CD68^{+} macrophage subset expanded in the myocardium of patients with COVID-19 (Figure 3C). More CD68^{+} macrophages accumulated and the CCR2^{+} CD68^{+} macrophage subset increase was more pronounced in patients with COVID-19 than in control cases regardless of the cause of death (Figure 3D and 3E), suggesting that SARS-CoV-2 infection led to a particularly strong cardiac immune response compared with other life-threatening diseases.

Anti-TNFα Antibody Therapy Improves Lung Inflammation in ^{VL}ARDS

We used the ^{VL}ARDS model to evaluate how anti-inflammatory therapies affect immune activation in mice with ^{VL}ARDS (Figure 4A). In an n=3 screening study, we administered daily injections of antibodies neutralizing IL1β, IL6, or TNFα, cytokines we found upregulated in ^{VL}ARDS. In addition, we used the dual CCR2/5 inhibitor cenicriviroc, which blocks monocyte recruitment and is currently being tested in patients with COVID-19.

On the basis of preliminary screening (Figure 4B; Table S2), we treated a larger ^{VL}ARDS cohort with TNFα-neutralizing antibodies, which preserved body weight and temperature (Figure 4C and 4D). This treatment did not improve lung opacity, as assayed with computed tomography (Figure 4E and 4F). However, anti-TNFα therapy improved blood oxygenation and survival (Figure 4G through 4I). CD45^{+} leukocyte recruitment into the lung was reduced in ^{VL}ARDS mice receiving anti-TNFα therapy (Figure 4J through 4L). This effect was mainly driven by lower neutrophil counts, whereas lung macrophage populations were comparable between study groups (Figure 4K). Anti-TNFα therapy decreased *Cxcl2*, *IL1β*, and *IL6* expression in lung tissue (Figure 4M), IL6 serum protein (Figure 4N), and Il6 and Il1ß protein in bronchoalveolar lavage fluid (Figure 4O). Taken together, these results indicate that targeting TNFα exerts beneficial effects in ARDS by ameliorating the host immune response.

Anti-TNFα Therapy Protects Cardiac Function in Mice With ^{VL}ARDS

Next, we tested whether anti-TNFα therapy limited the cardiac consequences of ^{VL}ARDS. We found that anti-TNFα therapy prevented ^{VL}ARDS-induced systolic dysfunction, as indicated by higher ejection fraction, stroke

Table. Baseline Characteristics of Clinical Cohort

Baseline characteristics	Controls	SARS-CoV-2 ARDS	*P* value
n	33	21	
Age	62.7 (57.8, 67.7)	64.3 (56.4, 72.1)	0.72
Male sex	17 (51.5%)	15 (71.4%)	0.16
BMI	26.6 (23.6, 29.7)	30.9 (25.1, 36.8)	0.15
Smoker			
Yes	1 (3%)	1 (4.8%)	>0.99
Former	12 (36.4%)	10 (47.6%)	>0.99
Never	15 (45%)	7 (33.3%)	0.41
Unknown	5 (15.2%)	3 (14.28)	>0.99
Primary cause of death			
Pulmonary	8 (24.3%)	19 (90.5%)	**<0.0001**
Cardiovascular	8 (24.3%)	1 (3%)	0.075
CNS	2 (6.1%)	0 (0%)	0.51
Other	14 (42.4)	1 (3%)	**0.004**
COVID-19 diagnosis*	0 (%)	21 (100%)	**<0.0001**
Mean time of death from diagnosis	…	20.8 (14.7, 26.8)	…
Clinical			
sO^2	94.7 (92.9, 96.5) (n=30)	91.5 (87.1, 95.9) (n=16)	0.32
Body temperature	36.7 (36.3, 37.0) (n=26)	37.0 (36.5, 37.5) (n=19)	0.44
Heart rate	89.9 (82.4, 97.4) (n=32)	103.4 (87.8, 119.0) (n=20)	0.077
Left ventricular ejection fraction	60.7 (56.0, 65.4) (n=24)	56.9 (49.1, 64.8) (n=14)	0.28
White blood cell count	16.9 (11.8, 22.0) (n=32)	18.3 (10.5, 26.0) (n=12)	0.46
Neutrophils	74.4 (68.1, 80.7) (n=28)	78.1 (73.1, 83.0) (n=19)	0.55
Lymphocytes	13.4 (8.7, 18.2) (n=28)	10.1 (6.7, 13.5) (n=19)	0.85
Monocytes	5.8 (4.6, 7.0) (n=26)	6.6 (5.5, 7.7) (n=19)	0.33

P values were calculated using a Fisher exact test (for categorical characteristics), unpaired parametric 2-tailed *t* test, or Mann-Whitney test (both for continuous characteristics), as appropriate. ARDS indicates acute respiratory distress syndrome; BMI, body mass index; and CNS, central nervous system.

volume, and cardiac output (Figure 5A and 5B). ^{VL}ARDS-induced cardiomyocyte apoptosis and cell recruitment to the myocardium appeared reduced in cardiac cross-sections (Figure 5C through 5E). Flow cytometry documented that this effect was driven by less monocyte influx (Figure 5F and 5G). Total cardiac macrophage counts trended lower and MHCII^{lo} CCR2^{+} and MHCII^{hi} CCR2^{-} macrophages were significantly less numerous if ^{VL}ARDS was treated with anti-TNFα antibodies (Figure 5H), which also lowered myocardial expression of *Il1β, Il6*, and *TNFα* (Figure 5I). Taken together, these results demonstrate that TNFα-neutralizing therapy curtailed lung and heart inflammation in mice with ^{VL}ARDS.

Pre-Existing Heart Failure With Preserved Ejection Fraction Associates With High Mortality in Mice With ^{VL}ARDS

The risk of dying from severe SARS-CoV-2 infection is 5 times higher in patients with pre-existing cardiovascular disease compared with patients without comorbidities.[31] To test whether ^{VL}ARDS recapitulates this clinical mortality, we exposed male mice with pre-existing heart failure with preserved ejection fraction (HFpEF) to ^{VL}ARDS. We induced HFpEF with hypertension and metabolic stress as recently described[32] (Figure 6A; Figure S6A and S6B). Echocardiography revealed preserved ejection fraction and diastolic dysfunction, as illustrated by increased E/A ratio, reduced E/e' ratio, and diminished global longitudinal peak strain (Figure 6B and 6C). Circulating neutrophils, monocytes, and Ly6C^{hi} monocytes were elevated in mice with HFpEF (Figure 6D), as has been observed in alternative HFpEF models.[33] HFpEF increased overall cardiac macrophages and the MHCII^{hi} Ccr2^{+} subset (Figure S6C). When naive controls and mice with HFpEF underwent ^{VL}ARDS induction (Figure 6E), pre-existing HFpEF further lowered body temperature and raised ^{VL}ARDS mortality (Figure 6F and 6G); inducing ^{VL}ARDS in mice with HFpEF lowered blood pressure (Figure S7A and S7B). We then assayed cardiac macrophages on day 3 after ^{VL}ARDS induction in mice with HFpEF, before the high mortality observed on day 4. We found that at this

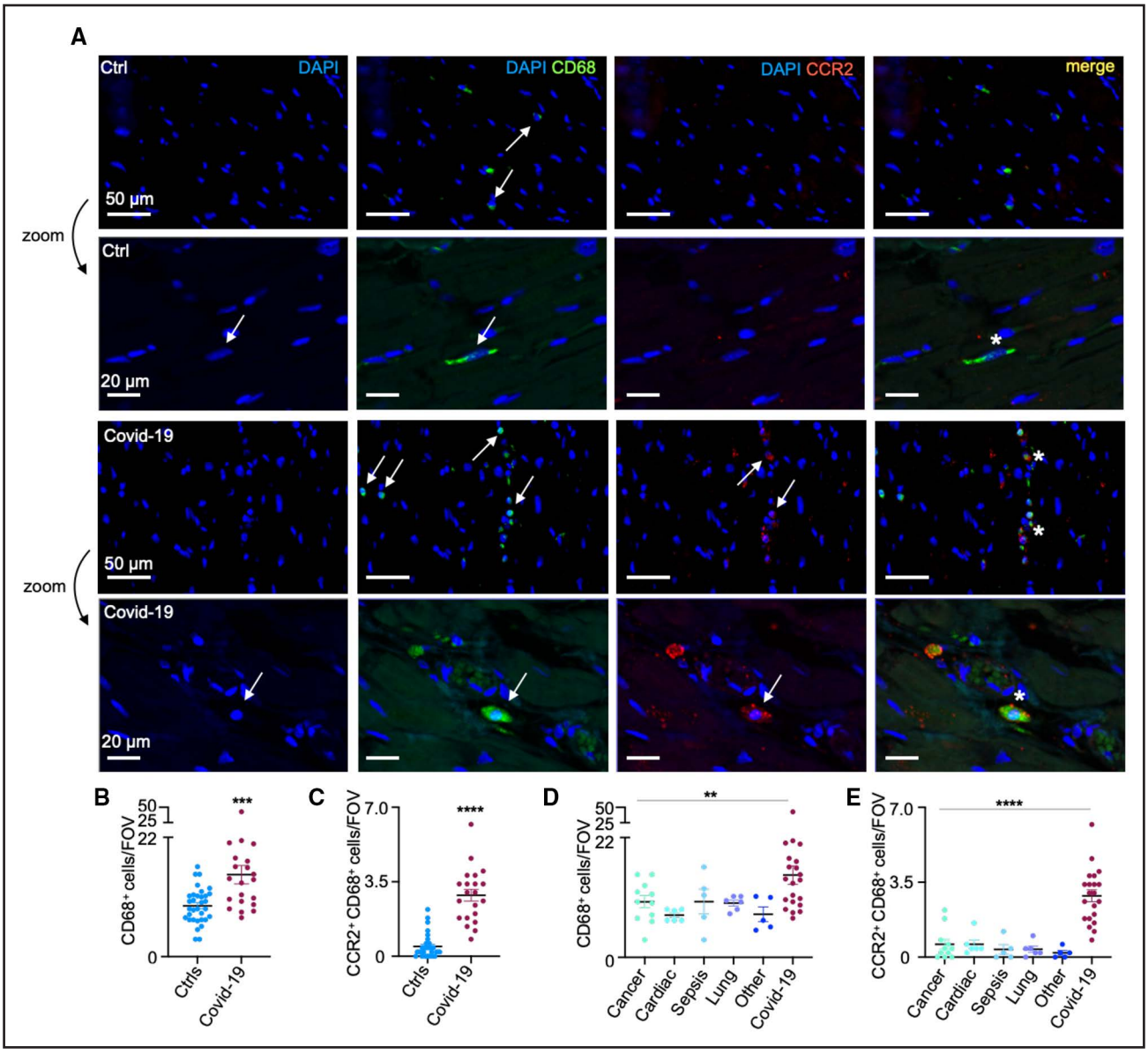

Figure 3. Human SARS-CoV-2–associated ARDS raises cardiac macrophage recruitment.
A, Immunofluorescence staining of myocardium from controls and patients with COVID-19. Tissue was stained with DAPI (blue), CD68-AF88 (green), and CCR2-DyLight 594 (red). Scale bar=50 µm or 20 µm, respectively. **B**, Quantification of CD68+ macrophages per field of view (FOV) and CCR2+ CD68+ macrophages (**C**) in controls and patients with COVID-19. **D**, CD68+ cells and CCR2+ CD68+ cells (**E**) per FOV stratified according to cause of death. ***P*<0.01; ****P*<0.001; *****P*<0.0001 vs control group. Mann-Whitney test or Kurskal-Wallis test followed by Dunn multiple comparisons test, as appropriate. Data are mean±SEM. ARDS indicates acute respiratory distress syndrome; and CCR2, C-C chemokine receptor type 2.

early time point, overall cardiac macrophage numbers declined in mice with HFpEF and ^{VL}ARDS, which was driven by lower numbers of MHCII^{hi} cells (Figure S7C). Finally, we examined whether anti-TNFα treatment was beneficial in mice with ^{VL}ARDS and HFpEF (Figure 6H). Indeed, anti-TNFα antibody injections preserved body temperature and decreased mortality compared with untreated ^{VL}ARDS mice with HFpEF (Figure 6I and 6J). This beneficial effect was associated with a reduced number of MHCII^{lo} Ccr2^{+} macrophages in the myocardium (Figure S8A and S8B).

DISCUSSION

Our article describes 2 novel insights: (1) SARS-CoV-2 infection shifts cardiac macrophage subsets toward the harmful, recruited CCR2^{+} phenotype in patients and mice, and (2) even in the absence of an actual virus, the host immune response to virus-like lung injury is sufficient to reproduce this heart macrophage subset shift (Figure S9). The relevance of deviating MHCII^{hi} Ccr2^{-} macrophage numbers in SARS-CoV-2–infected versus ^{VL}ARDS mice remains to be explored. TNFα-neutralizing

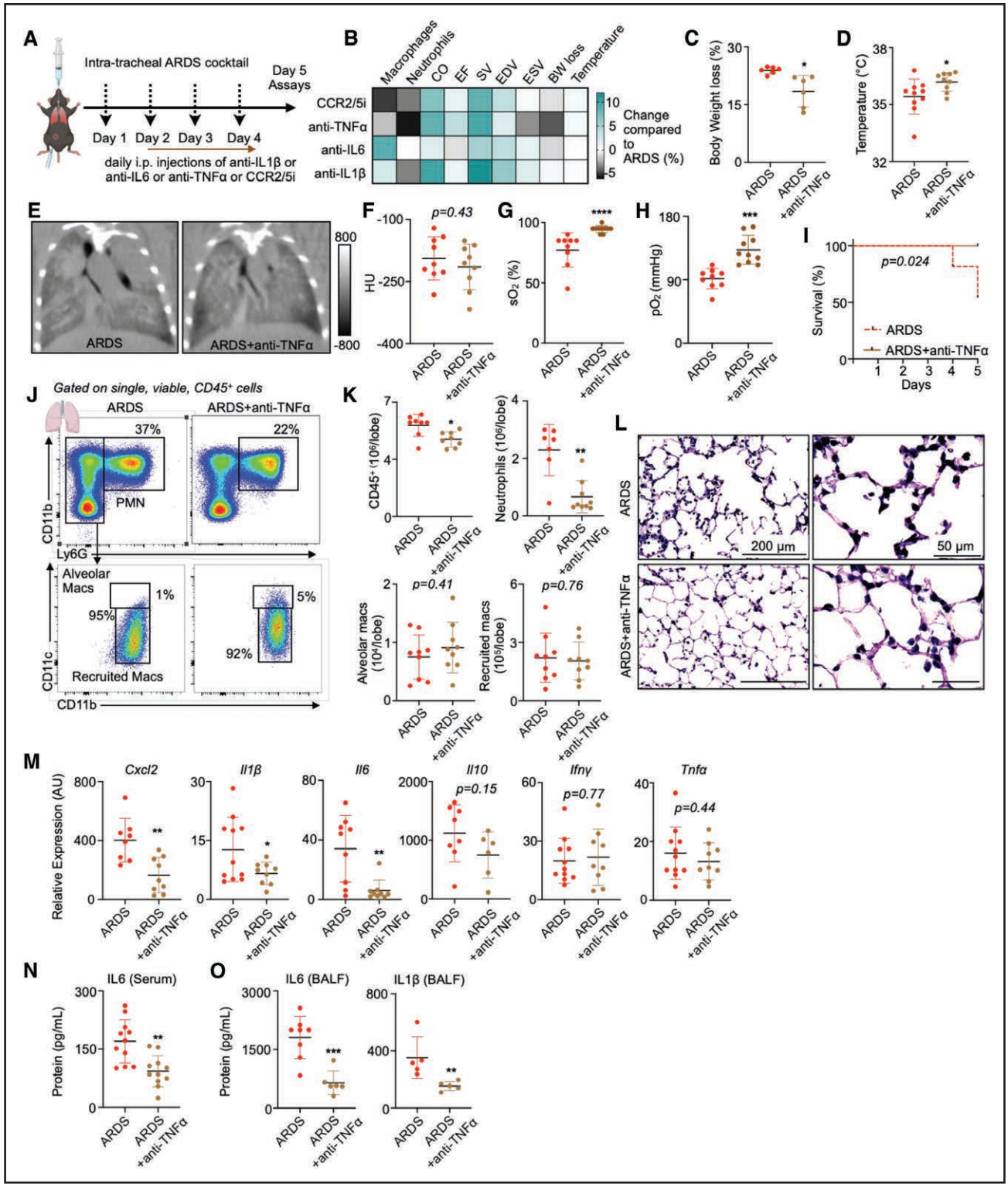

Figure 4. Anti-TNFα therapy protects against ^{VL}ARDS.

A, Experimental outline of anti-inflammatory drug screen. All readouts were taken on day 5 after the first instillation. **B**, Heat map indicating readouts of drug screen expressed as percentage change compared with the average of untreated ^{VL}ARDS mice (%; n=3 mice per group; leukocytes were enumerated in the heart. **C**, Body weight loss (%). **D**, Body temperature (°C). **E**, Computed tomography images and quantification of lung opacity (**F**) in Hounsfield units (HU). **G**, sO2 and PaO2 (**H**) in arterial blood. **I**, Kaplan-Meier curve indicating mortality of ^{VL}ARDS (n=11) and ^{VL}ARDS in mice treated with anti-TNFα antibody (n=10 mice, log-rank Mantel-Cox test). **J**, Representative flow plots of lung tissue and quantification of leukocytes, neutrophils, and macrophages (**K**) per lung lobe. **L**, H&E staining of lung tissue. Scale bar=200 µm (**left**) or 50 µm (**right**). **M**, Gene expression analysis in lung tissue. **N**, ELISA for IL6 in serum. **O**, ELISA for IL6 and IL-1ß in bronchoalveolar lavage fluid (BALF). *P<0.05; **P<0.01; ***P<0.001 vs ^{VL}ARDS group. Unpaired parametric 2-tailed t test or Mann-Whitney test, as appropriate. Data are mean±SEM. ARDS indicates acute respiratory distress syndrome; CCR2, C-C chemokine receptor type 2; and ^{VL}ARDS, virus-like ARDS.

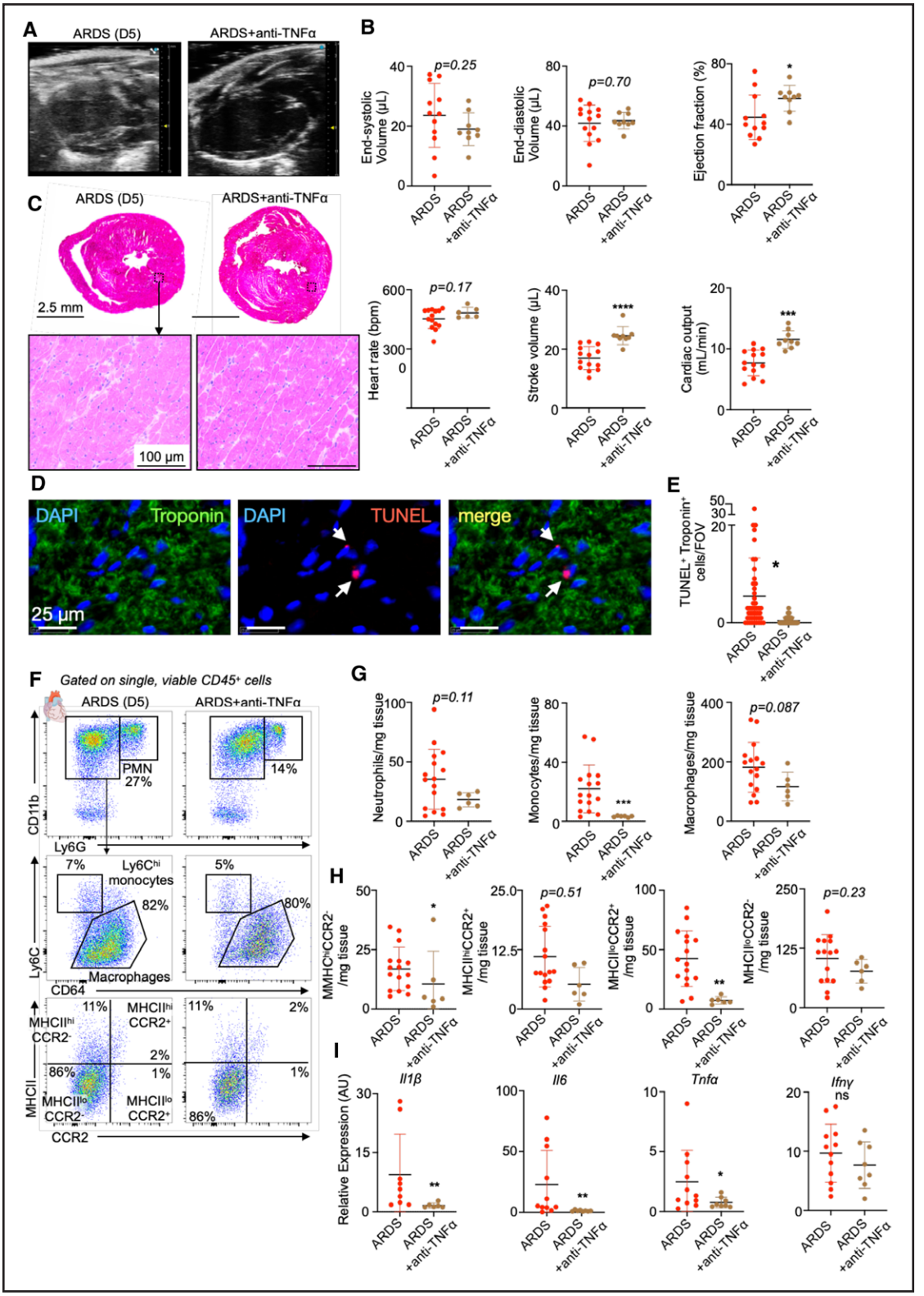

Figure 5. Anti-TNFα therapy prevents ARDS-induced changes in macrophage subsets and improves cardiac function.
A, B-mode images in a parasternal long-axis view and analyses of left ventricular systolic function (**B**). **C**, H&E-stained cardiac cross-sections and 20× magnifications, demonstrating cellular infiltrations. Scale bar=2.5 mm (**top**) or 100 µm (**bottom**). **D**, Representative images from cardiac cross-sections stained with DAPI (blue), troponin (green), and TUNEL (red); scale bars=25 µm. **E**, Quantification of troponin⁺ TUNEL⁺ cells. Nested *t* test. **F**, Representative flow plots of cardiac tissue and (**G**) corresponding quantification of leukocytes and (**H**) macrophage subsets, based on CCR2 and MHCII. **I**, qRT-PCR analysis of heart tissue. **P*<0.05; ***P*<0.01; ****P*<0.001; *****P*<0.0001 vs ^{VL}ARDS group. Unpaired parametric 2-tailed *t* test or Mann-Whitney test, as appropriate. Data are mean±SEM. ARDS indicates acute respiratory distress syndrome; CCR2, C-C chemokine receptor type 2; and ^{VL}ARDS, virus-like ARDS.

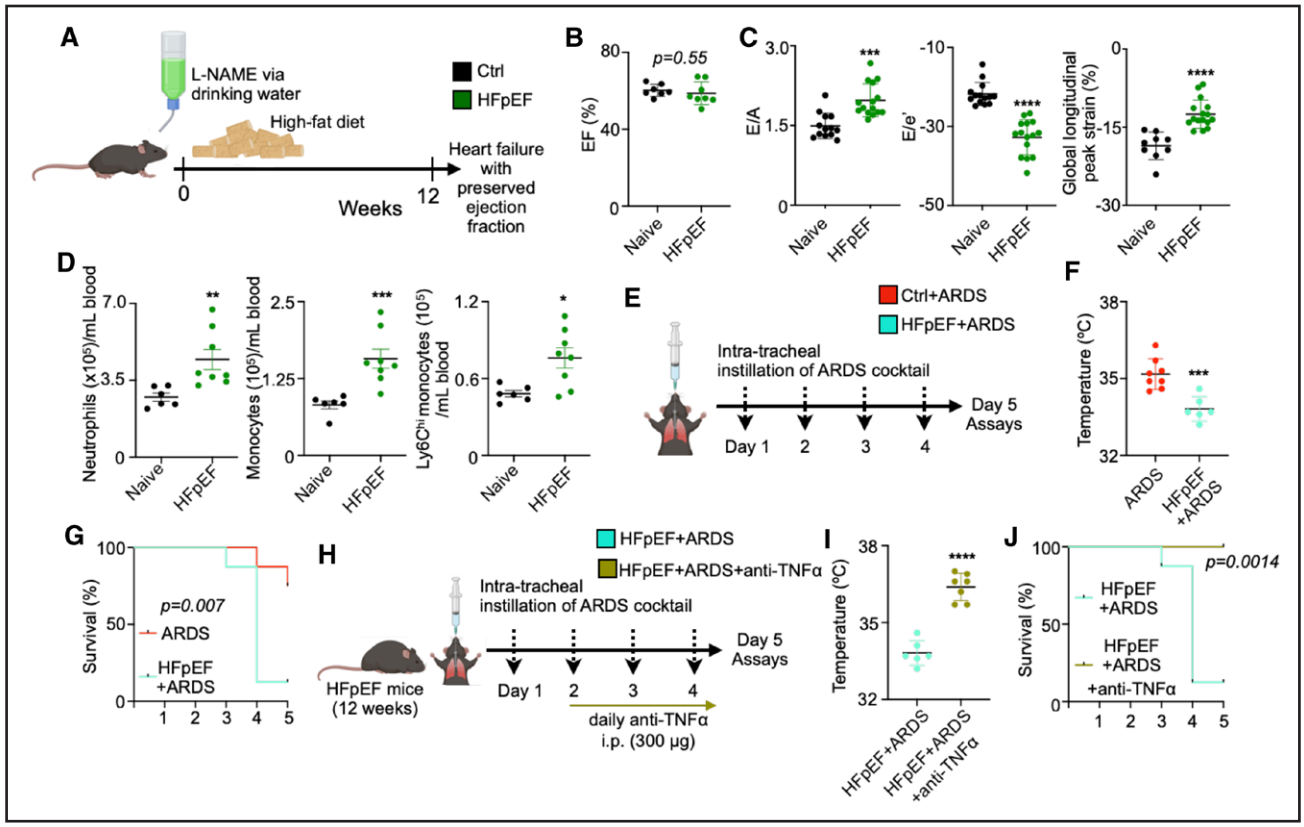

Figure 6. Pre-existing HFpEF increases ^{VL}ARDS mortality.
A, Experimental outline of inducing heart failure with preserved ejection fraction (HFpEF) in mice by L-NAME (drinking water) and 60% high-fat diet, both ad libitum over 12 weeks. **B**, Echocardiographic assessment of ejection fraction (EF) and diastolic function (**C**), indicated by the late diastolic transmitral flow velocity (E/A), the ratio between mitral inflow velocity and mitral valve annular early diastolic velocity (E/e'), and the global longitudinal peak strain (GLS). **D**, Blood leukocyte numbers assessed by flow cytometry in naive controls and mice with HFpEF. **E**, Experimental outline of ^{VL}ARDS induction in naive mice (Ctrl) and mice with pre-existing HFpEF. **F**, Body temperature (°C) measured on day 4 after first intratracheal instillation. **G**, Kaplan-Meier curve indicating mortality of ^{VL}ARDS (n=11) and HFpEF+^{VL}ARDS (n=8) mice. **H**, Experimental outline indicating treatment of HFpEF+ARDS mice with anti-TNFα therapy. **I**, Body temperature (°C) measured on day 4 after first intratracheal instillation. **J**, Kaplan-Meier curve indicating mortality of HFpEF+^{VL}ARDS (n=8) and HFpEF+^{VL}ARDS+anti-TNFα treatment (n=8, log-rank Mantel-Cox test).*P<0.05; ***P<0.001; and ****P<0.0001 vs naive group (**C** and **D**), vs ^{VL}ARDS group (**F**), or vs HFpEF+^{VL}ARDS (**I**). Unpaired parametric 2-tailed t test or Mann-Whitney test, as appropriate. Data are mean±SEM. ARDS indicates acute respiratory distress syndrome; and ^{VL}ARDS, virus-like ARDS.

antibodies inhibited some of these macrophage subset alterations and the associated cardiac functional decline. Our findings indicate that systemic and myocardial inflammatory signals elicited by virally induced ARDS may contribute to the cardiovascular complications and high mortality rates of this condition. In addition, our study confirms previous reports[9] that SARS-CoV-2 infection increases overall macrophage numbers in human hearts.

In the healthy myocardium, macrophages perform important housekeeping functions, including mitochondrial pruning to preserve the metabolic integrity of cardiomyocytes by outsourced autophagy.[27] We speculate that a phenotypic shift toward inflammatory macrophage subsets could compromise essential housekeeping functions, leading to metabolically challenged cardiomyocytes and reduced cardiac function. Given that cardiovascular pathologies are part of a protracted recovery in long-haul COVID-19, future studies should explore how altered immune cell landscapes in the heart contribute to this syndrome.

Systemic effects of bacterial or viral infections causing cardiac dysfunction have been described in patients with sepsis.[34] Although molecular mechanisms of sepsis-induced myocardial dysfunction remain incompletely understood, TLR4 signaling, as included in our model by LPS challenge, is a well-accepted driver of myocardial dysfunction.[35] Our data indicate that myocardial neutrophil recruitment in ARDS is TLR4-dependent. If ARDS-related TLR4 signaling also directly affects cardiac macrophages or other cells expressing TLRs (eg, cardiomyocytes) is less clear.

In patients with ARDS, sepsis, or SARS-CoV-2 infection, cardiac function can be compromised, especially if pre-existing cardiovascular conditions are present and if ventilation is required.[36] In isolation or combined, comorbidities like hyperlipidemia, obesity, or hypertension

increase the risk of death in patients with ARDS.[37] We speculate that the observed effects on cardiac macrophage numbers and phenotypes may contribute to the worse prognoses of patients with ARDS. Inflammatory macrophage phenotypes propel atherosclerosis and heart failure; hence, altered cardiac macrophage subsets as seen in our study may support disease progression and poor outcome.

Study limitations include that our experiments induced ^{VL}ARDS in young mice, a protocol that simplified the complex clinical situations of older patients with various comorbidities. Our clinical data do not include potential effects of COVID-19 vaccines because all human specimens were collected before vaccinations became available. Although our data indicate that viral presence is not necessary for cardiac injury in mice with ^{VL}ARDS, viral infection likely has additional influence on the heart and immune system. Thus, there are likely many potentially important differences between ^{VL}ARDS and SARS-CoV-2–infected mice, including but not limited to myocardial IFNγ and TNFα expression. Previous data in mice with sepsis reveal that heart macrophage numbers expand because of enhanced cell recruitment and proliferation.[38] During bacteremia, cardiac resident macrophages phagocytosed bacteria and died as a consequence,[38] also shifting the predominant cardiac macrophage phenotype away from protective and toward harmful inflammatory subsets, as in our current work. The precise reason for the initial decline of cardiac resident macrophages remains to be uncovered. Given the converging theme of initial tissue macrophage rarefaction in systemic inflammation, these results warrant broader phenotyping (eg, by whole transcriptome assays) of cardiac macrophages and other heart leukocytes after ^{VL}ARDS or infection to obtain a more complete picture of immune pathway contributions to cardiac complications.

Our study indicates that cardiac macrophage subsets change in patients with COVID-19. Given what is known about the crucial roles cardiac macrophages play in myocardial ischemia, heart failure, and myocarditis, this observation suggests that cardiac leukocytes should be considered a therapeutic target to alleviate cardiovascular complications in vulnerable patients with viral infections. Macrophage subset depletion studies are needed to test this hypothesis. Our data acquired in mice with ^{VL}ARDS support the idea that depleting neutrophils or neutralizing TNFα may alleviate inflammatory cardiac complications. Several clinical trials are currently testing immunomodulation in severe COVID-19. First results of a randomized clinical indicate that TNFα inhibition with infliximab may reduce COVID-19 mortality, although a predefined end point, time to recovery, was not significantly affected by the treatment.[39] Our data obtained in mice with HFpEF support that specific patient subgroups, perhaps even those with coexisting cardiovascular pathologies, may benefit from such treatment. However, especially in the setting of active infection, such considerations must take into account that innate immune cells remove pathogens, and that their depletion will likely impede bacterial and viral clearance.

ARTICLE INFORMATION

Received July 20, 2023; accepted February 15, 2024.

Affiliations

Center for Systems Biology (J.G., G.B., P.T.O., K.M., S.P., N.K., F.E.P., D.R., S.Z., Y.I., G.R.W., C.V., M.H., M.N.), Department of Radiology (J.G., G.B., P.T.O., K.M., S.P., N.K., F.E.P., D.R., S.Z., C.V., M.H., M.N.), Department of Pathology, Center for Integrated Diagnostics (U.G., J.K.L.), Massachusetts General Hospital and Harvard Medical School, Boston. Department of Cardiothoracic and Vascular Surgery, Deutsches Herzzentrum Der Charité, Berlin, Germany (J.G.). Charité–Universitätsmedizin Berlin, Corporate Member of Freie Universität Berlin and Humboldt-Universität Zu Berlin, Institute of Physiology, Germany (J.G.). German Center for Cardiovascular Research, Partner Site Berlin (J.G.). Department of Cardiology, University Hospital Heidelberg, Germany (P.T.O.). Meakins-Christie Laboratories, Department of Medicine, Department of Microbiology and Immunology, Department of Pathology, Research Institute McGill University Health Centre, and McGill International TB Centre Montreal, Canada (E.K., K.A.T., M.D.). Department of Biomedical and Molecular Sciences, Queen's University, Kingston, Canada (E.K.). Department of Internal Medicine II, University Medical Center Regensburg, Germany (S.P.). Department of Internal Medicine I, University Hospital Aachen, RWTH Aachen University, Germany (N.K.). Cardiovascular Research Institute, Icahn School of Medicine at Mount Sinai, New York, NY (F.K.S.). Department of Pathology (J.R.S.), Gordon Center for Medical Imaging (M.N.), Massachusetts General Hospital, Boston (J.R.S.). Department of Internal Medicine, University Hospital Wuerzburg, Germany (M.N.).

Acknowledgments

The authors acknowledge Kaley Joyes for editing the article and Niklas Hegemann for technical support in processing ECG data. Cartoons were created with BioRender (publication license HU25JUQA72).

Sources of Funding

This work was funded in part by US federal funds HL139598, HL142494, HL155097, HL149647, HL166538, and HL157073. J.G. was funded by the Deutsche Forschungsgemeinschaft (German Research Foundation; SFB-1470 A04 and GR 5261/1-1), Corona-Stiftung Grant (S199/10086/2022), the German Society for Cardiology, and the German Center for Cardiovascular Research. M.D. was supported by a Canadian Institutes of Health research project grant (MM1-174910).

Disclosures

M.N. has received funds or material research support from Alnylam, Biotronik, CSL Behring, GlycoMimetics, GSK, Medtronic, Novartis, and Pfizer, as well as consulting fees from Lilly, Biogen, Gimv, IFM Therapeutics, Molecular Imaging, Sigilon, and Verseau Therapeutics. The other authors report no conflicts.

Supplemental Material

Supplemental Methods
Tables S1–S2
Figures S1–S9

REFERENCES

1. Bos LDJ, Sjoding M, Sinha P, Bhavani SV, Lyons PG, Bewley AF, Botta M, Tsonas AM, Serpa Neto A, Schultz MJ, et al. Longitudinal respiratory subphenotypes in patients with COVID-19-related acute respiratory distress syndrome: results from three observational cohorts. *Lancet Respir Med.* 2021;9:1377–1386. doi: 10.1016/S2213-2600(21)00365-9
2. Yang L, Xie X, Tu Z, Fu J, Xu D, Zhou Y. The signal pathways and treatment of cytokine storm in COVID-19. *Signal Transduct Target Ther.* 2021;6:255. doi: 10.1038/s41392-021-00679-0
3. Metkus TS, Sokoll LJ, Barth AS, Czarny MJ, Hays AG, Lowenstein CJ, Michos ED, Nolley EP, Post WS, Resar JR, et al. Myocardial injury in severe COVID-19 compared with non-COVID-19 acute respiratory distress syndrome. *Circulation.* 2021;143:553–565. doi: 10.1161/CIRCULATIONAHA.120.050543

4. Xie Y, Xu E, Bowe B, Al-Aly Z. Long-term cardiovascular outcomes of COVID-19. *Nat Med*. 2022;28:583–590. doi: 10.1038/s41591-022-01689-3
5. Nicholls JM, Poon LL, Lee KC, Ng WF, Lai ST, Leung CY, Chu CM, Hui PK, Mak KL, Lim W, et al. Lung pathology of fatal severe acute respiratory syndrome. *Lancet*. 2003;361:1773–1778. doi: 10.1016/s0140-6736(03)13413-7
6. Liao M, Liu Y, Yuan J, Wen Y, Xu G, Zhao J, Cheng L, Li J, Wang X, Wang F, et al. Single-cell landscape of bronchoalveolar immune cells in patients with COVID-19. *Nat Med*. 2020;26:842–844. doi: 10.1038/s41591-020-0901-9
7. Bajpai G, Schneider C, Wong N, Bredemeyer A, Hulsmans M, Nahrendorf M, Epelman S, Kreisel D, Liu Y, Itoh A, et al. The human heart contains distinct macrophage subsets with divergent origins and functions. *Nat Med*. 2018;24:1234–1245. doi: 10.1038/s41591-018-0059-x
8. Epelman S, Lavine KJ, Beaudin AE, Sojka DK, Carrero JA, Calderon B, Brija T, Gautier EL, Ivanov S, Satpathy AT, et al. Embryonic and adult-derived resident cardiac macrophages are maintained through distinct mechanisms at steady state and during inflammation. *Immunity*. 2014;40:91–104. doi: 10.1016/j.immuni.2013.11.019
9. Basso C, Leone O, Rizzo S, De Gaspari M, van der Wal AC, Aubry MC, Bois MC, Lin PT, Maleszewski JJ, Stone JR. Pathological features of COVID-19-associated myocardial injury: a multicentre cardiovascular pathology study. *Eur Heart J*. 2020;41:3827–3835. doi: 10.1093/eurheartj/ehaa664
10. Di Domizio J, Gulen MF, Saidoune F, Thacker VV, Yatim A, Sharma K, Nass T, Guenova E, Schaller M, Conrad C, et al. The cGAS-STING pathway drives type I IFN immunopathology in COVID-19. *Nature*. 2022;603:145–151. doi: 10.1038/s41586-022-04421-w
11. Kuba K, Imai Y, Rao S, Gao H, Guo F, Guan B, Huan Y, Yang P, Zhang Y, Deng W, et al. A crucial role of angiotensin converting enzyme 2 (ACE2) in SARS coronavirus-induced lung injury. *Nat Med*. 2005;11:875–879. doi: 10.1038/nm1267
12. Sui Y, Li J, Venzon DJ, Berzofsky JA. SARS-CoV-2 spike protein suppresses ACE2 and type I interferon expression in primary cells from macaque lung bronchoalveolar lavage. *Front Immunol*. 2021;12:658428. doi: 10.3389/fimmu.2021.658428
13. Dos Santos CC, Slutsky AS. Invited review: mechanisms of ventilator-induced lung injury: a perspective. *J Appl Physiol (1985)*. 2000;89:1645–1655. doi: 10.1152/jappl.2000.89.4.1645
14. Matute-Bello G, Frevert CW, Martin TR. Animal models of acute lung injury. *Am J Physiol Lung Cell Mol Physiol*. 2008;295:L379–L399. doi: 10.1152/ajplung.00010.2008
15. Zou X, Chen K, Zou J, Han P, Hao J, Han Z. Single-cell RNA-seq data analysis on the receptor ACE2 expression reveals the potential risk of different human organs vulnerable to 2019-nCoV infection. *Front Med*. 2020;14:185–192. doi: 10.1007/s11684-020-0754-0
16. Hoffmann M, Kleine-Weber H, Schroeder S, Krüger N, Herrler T, Erichsen S, Schiergens TS, Herrler G, Wu NH, Nitsche A, et al. SARS-CoV-2 cell entry depends on ACE2 and TMPRSS2 and is blocked by a clinically proven protease inhibitor. *Cell*. 2020;181:271–280.e8. doi: 10.1016/j.cell.2020.02.052
17. Imai Y, Kuba K, Rao S, Huan Y, Guo F, Guan B, Yang P, Sarao R, Wada T, Leong-Poi H, et al. Angiotensin-converting enzyme 2 protects from severe acute lung failure. *Nature*. 2005;436:112–116. doi: 10.1038/nature03712
18. De Mello WC, Danser AH. Angiotensin II and the heart: on the intracrine renin-angiotensin system. *Hypertension*. 2000;35:1183–1188. doi: 10.1161/01.hyp.35.6.1183
19. Kao KC, Chiu LC, Hung CY, Chang CH, Yang CT, Huang CC, Hu HC. Coinfection and mortality in pneumonia-related acute respiratory distress syndrome patients with bronchoalveolar lavage: a prospective observational study. *Shock*. 2017;47:615–620. doi: 10.1097/SHK.0000000000000802
20. Fontes-Dantas FL, Fernandes GG, Gutman EG, De Lima EV, Antonio LS, Hammerle MB, Mota-Araujo HP, Colodeti LC, Araujo SMB, Froz GM, et al. SARS-CoV-2 spike protein induces TLR4-mediated long-term cognitive dysfunction recapitulating post-COVID-19 syndrome in mice. *Cell Rep*. 2023;42:112189. doi: 10.1016/j.celrep.2023.112189
21. Manik M, Singh RK. Role of toll-like receptors in modulation of cytokine storm signaling in SARS-CoV-2-induced COVID-19. *J Med Virol*. 2022;94:869–877. doi: 10.1002/jmv.27405
22. Máca J, Jor O, Holub M, Sklienka P, Burša F, Burda M, Janout V, Ševčík P. Past and present ARDS mortality rates: a systematic review. *Respir Care*. 2017;62:113–122. doi: 10.4187/respcare.04716
23. Holt PG, Strickland DH, Wikström ME, Jahnsen FL. Regulation of immunological homeostasis in the respiratory tract. *Nat Rev Immunol*. 2008;8:142–152. doi: 10.1038/nri2236
24. Moore JB, June CH. Cytokine release syndrome in severe COVID-19. *Science*. 2020;368:473–474. doi: 10.1126/science.abb8925
25. Merad M, Martin JC. Pathological inflammation in patients with COVID-19: a key role for monocytes and macrophages. *Nat Rev Immunol*. 2020;20:355–362. doi: 10.1038/s41577-020-0331-4
26. Chang WT, Toh HS, Liao CT, Yu WL. Cardiac involvement of COVID-19: a comprehensive review. *Am J Med Sci*. 2021;361:14–22. doi: 10.1016/j.amjms.2020.10.002
27. Nicolás-Ávila JA, Lechuga-Vieco AV, Esteban-Martínez L, Sánchez-Díaz M, Díaz-García E, Santiago DJ, Rubio-Ponce A, Li JL, Balachander A, Quintana JA, et al. A network of macrophages supports mitochondrial homeostasis in the heart. *Cell*. 2020;183:94–109.e23. doi: 10.1016/j.cell.2020.08.031
28. Grune J, Lewis AJM, Yamazoe M, Hulsmans M, Rohde D, Xiao L, Zhang S, Ott C, Calcagno DM, Zhou Y, et al; Oxford Acute Myocardial Infarction (OxAMI) Study. Neutrophils incite and macrophages avert electrical storm after myocardial infarction. *Nat Cardiovasc Res*. 2022;1:649–664. doi: 10.1038/s44161-022-00094-w
29. Bajpai G, Bredemeyer A, Li W, Zaitsev K, Koenig AL, Lokshina I, Mohan J, Ivey B, Hsiao HM, Weinheimer C, et al. Tissue resident CCR2- and CCR2+ cardiac macrophages differentially orchestrate monocyte recruitment and fate specification following myocardial injury. *Circ Res*. 2019;124:263–278. doi: 10.1161/CIRCRESAHA.118.314028
30. Wijdeven RH, van Luijn MM, Wierenga-Wolf AF, Akkermans JJ, van den Elsen PJ, Hintzen RQ, Neefjes J. Chemical and genetic control of IFNgamma-induced MHCII expression. *EMBO Rep*. 2018;19:e45553. doi: 10.15252/embr.201745553
31. Wu Z, McGoogan JM. Characteristics of and important lessons from the coronavirus disease 2019 (COVID-19) outbreak in China: summary of a report of 72 314 cases from the Chinese Center for Disease Control and Prevention. *JAMA*. 2020;323:1239–1242. doi: 10.1001/jama.2020.2648
32. Schiattarella GG, Altamirano F, Tong D, French KM, Villalobos E, Kim SY, Luo X, Jiang N, May HI, Wang ZV, et al. Nitrosative stress drives heart failure with preserved ejection fraction. *Nature*. 2019;568:351–356. doi: 10.1038/s41586-019-1100-z
33. Hulsmans M, Sager HB, Roh JD, Valero-Munoz M, Houstis NE, Iwamoto Y, Sun Y, Wilson RM, Wojtkiewicz G, Tricot B, et al. Cardiac macrophages promote diastolic dysfunction. *J Exp Med*. 2018;215:423–440. doi: 10.1084/jem.20171274
34. Shvilkina T, Shapiro N. Sepsis-induced myocardial dysfunction: heterogeneity of functional effects and clinical significance. *Front Cardiovasc Med*. 2023;10:1200441. doi: 10.3389/fcvm.2023.1200441
35. Nemoto S, Vallejo JG, Knuefermann P, Misra A, Defreitas G, Carabello BA, Mann DL. Escherichia coli LPS-induced LV dysfunction: role of Toll-like receptor-4 in the adult heart. *Am J Physiol Heart Circ Physiol*. 2002;282:H2316–H2323. doi: 10.1152/ajpheart.00763.2001
36. Formenti P, Coppola S, Massironi L, Annibali G, Mazza F, Gilardi L, Pozzi T, Chiumello D. Left ventricular diastolic dysfunction in ARDS patients. *J Clin Med*. 2022;11:5998. doi: 10.3390/jcm11205998
37. de Araujo MFM, Monteiro FPM, de Araujo TM, Lira Neto JCG, Santos LFS, Rolim ILTP, Santos FS, Pascoal LM, Costa ACPJ, Santos Neto M. Individual and mutual effects of diabetes, hypertension, and obesity on acute respiratory distress syndrome mortality rates in clinical patients: a multicentre study. *Front Public Health*. 2023;11:1219271. doi: 10.3389/fpubh.2023.1219271
38. Hoyer FF, Naxerova K, Schloss MJ, Hulsmans M, Nair AV, Dutta P, Calcagno DM, Herisson F, Anzai A, Sun Y, et al. Tissue-specific macrophage responses to remote injury impact the outcome of subsequent local immune challenge. *Immunity*. 2019;51:899–914.e7. doi: 10.1016/j.immuni.2019.10.010
39. O'Halloran JA, Ko ER, Anstrom KJ, Kedar E, McCarthy MW, Panettieri RAJ, Maillo M, Nunez PS, Lachiewicz AM, Gonzalez C, et al; ACTIV-1 IM Study Group Members. Abatacept, cenicriviroc, or infliximab for treatment of adults hospitalized with COVID-19 pneumonia: a randomized clinical trial. *JAMA*. 2023;330:328–339. doi: 10.1001/jama.2023.11043